

Fabrication of electrical microfluidic chip for electroporation of mammalian cells

Mehdi Shahini*, Frans van Wijngaarden** and John T.W. Yeow***

* Systems Design Engineering, University of Waterloo, Canada, m2shahin@uwaterloo.ca

**MESA+ Institute for Nanotechnology, University of Twente, The Netherlands,
f.vanwijngaarden@student.utwente.nl

***Corresponding author, Systems Design Engineering, University of Waterloo, Canada,
jyeow@uwaterloo.ca

Fax: +1 519 746-4791; Tel: +1 519 888-4567 Ext. 32152

ABSTRACT

In this research, we demonstrate a novel method of creating microfluidic channels with electrical capabilities. The goal is to develop a process to create such chips that is low-cost, high-speed and very adaptable, while still being useful for a wide array of microfluidic-based systems, including cell manipulation devices. Through the use of a CO₂ laser, we develop a method that allows quick creation of versatile microfluidic chips with electrical functionalities. By bonding our microfluidic channels with glass that is coated with a transparent conductor Indium tin oxide (ITO), we achieved chip-wide electrodes with minimal extra effort. The added benefit is transparency, thereby allowing in-situ monitoring of the microfluidic channel by a wide variety of optical techniques. To test the performance of the proposed methodology, we have performed single cell electroporation on Chinese hamster ovary (CHO) cells, as a sample of mammalian cells.

Keywords: microfluidic channel, electroporation, laser, polyimide, cell lysis

1 INTRODUCTION

Microfluidic chips have been in use for well over a decade, and for a wide variety of applications [1–4]. Because most microfluidic chips are designed to be disposables, polymers are highly popular as a material. They are low-cost, and come in a wide variety of specifications [5]. Often-used polymers are SU-8 [6], PMMA [1], PDMS [7] and Polyimide [8]. Bonding is either done using the same polymer, or using an external layer. Electrodes can be integrated, but require extra steps and often are opaque to visible light. Popular fabrication methods are lithography, laser-ablation (often done using high-resolution excimer lasers) or embossing (especially useful for fabricating large numbers of identical microfluidic chips).

In this research, we used a combination of DuPont's Kapton polyimide with ITO-coated glass slides to create microfluidic chips, while using a CO₂ laser engraving machine to ablate the channel design in the polyimide. Kapton is a sheet of polyimide with FEP adhesive already coated on both sides. This allows simple bonding to glass

by heating the FEP while applying pressure. ITO as a conductive material enables an electric field in the channel while its optical transparency allows microscopy techniques to be utilized in characterizing the behavior of the microfluidic chip. Although all these techniques have been used before individually in the creation of microfluidic channels, this is the first time these techniques have been used together to create a low-cost, high-speed and highly adaptable method of making microfluidic chips with electrical capabilities.

2 FABRICATION METHODOLOGY

In the presented methodology, the microchannel pattern is cut out of polyimide using a CO₂ laser engraving machine, and bonded to two ITO-coated glass substrates using Teflon as an adhesion layer. The laser machine is capable of engraving any desired design, so creation of different channels is straightforward. By using ready-made polyimide sheets with Teflon coating (DuPont's Kapton brand), bonding becomes a simple process requiring only a pressure vice and a vacuum oven. A sample of polyimide sheet bonded to ITO-coated glass slides is depicted in Figure 1.

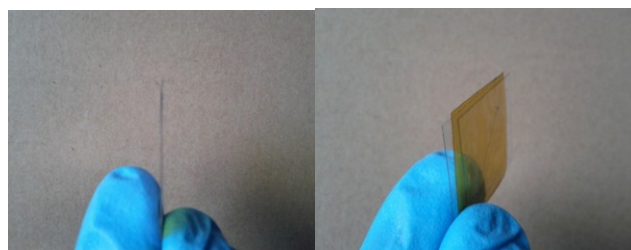


Figure 1 laser-ablated polyimide sandwiched between two ITO-coated coverslips

For fabrication, we used a CO₂ laser engraver to ablate a channel completely through the Kapton. Next, we cap this channel by ITO-coated glass slides on both sides. Thus, the height of the channel is determined by the thickness of the Kapton sheet used, the minimum width is determined by the minimum resolution of the laser machine, and by its spot size. The CO₂ laser is also used to drill holes through the ITO-coated glass, allowing access to the channels. The

channel design is free to chose, and easily adaptable between chips. A snapshot of the whole chip is shown in Figure 2.

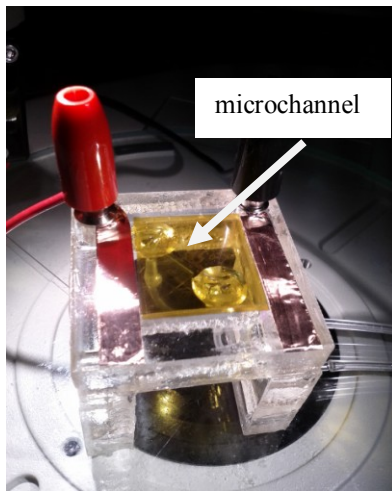


Figure 2 Snapshot of microchannel on a chip holder. A channel with 200 μm width and 50- μm height is confined with ITO-coated substrates. The fluidic tubes are connected through the bottom side.

The use of a CO₂ laser is cheap and safe, requiring none of the toxic gasses often used for excimer lasers. Both the power and the speed need to be controlled, since having these too high causes the heat affected zone to be too large, resulting in very poor resolution. The settings are shown in Table 1.

Table 1 Laser settings for different components of microchip

Material	Thickness (mm)	Power (mW)	Speed (mm/s)	No of iterations
Kapton Polyimide	0.05	30	0.25	3
ITO-coated microscope slide	1.1	1500	0.5	10

The separate pieces are bonded together using the FEP adhesive already applied to the polyimide. To bind this, the entire stack must be put under pressure and heated to 280 deg C. This is done by placing the chip inside a small vise, and using a vacuum oven to melt the FEP. This process must be done slowly, since if the thermal gradient is too high, the ITO-coated glass slides will crack. This can ruin the electrical contact between the ITO at the channel and the exposed ITO to the side. The ITO can also crack by an

uneven pressure distribution inside the vise. To counter this, a set of additional vise jaws were made by wrapping a small piece of thermal blanket, together with a glass microscopy slide, around aluminum foil. This evened out the pressure across the microscopy slide, preventing local spikes from cracking the glass. After bonding, syringe tips were glued to the chip to allow pumping of fluid into the microfluidic channel. These were glued to the bottom side, keeping the optical transparency on the top side intact.

3 ELECTROPORATION EXPERIMENT

The performance of the chip was tested on irreversible single-cell scale electroporation which requires relatively high voltages. CHO cells were pumped to the microchannel to experience electric field. Cells were loaded with a fluorogenic dye, Calcein AM, and the electroporation of each was individually recorded in real-time via fluorescent microscopy. The fluorescent Calcein compound flows out of the cell when an applied electrical field results in pores being created across the cell membrane. Electroporation is quantified by image analysis of cells with leaked intracellular materials. By customizing of ITO electrodes and the design of microchannel pattern, utilization and integration of the proposed electrical microchannel in variety of other MEMS-based devices are achievable.

To determine the usability of our fabrication method, the electroporation of single cells was used as an experimental setup. For this, Chinese Hamster Ovary (CHO) cells were used while suspended in a phosphate-sucrose buffer. The cells were loaded with Calcein-AM compound. The non-fluorescent Calcein-AM is permeable to cell membranes, and hydrolyzes inside the cell to the membrane-impermeable fluorescent Calcein compound. Thus, by observing the fluorescent intensity of the cells when exposed to the electrical field, cell electroporation could be observed.

The applied electrical field was a symmetric block-wave AC signal at 1 kHz, with an amplitude up to 5V. Electroporation of CHO cells happens when the potential drop across the membrane is large enough. If the potential is high enough, pores will occur through the membrane. The membrane-impermeable Calcein compound can flow out of the cells through these pores, thereby decreasing the fluorescent intensity of the cell when electroporation occurs.

4 RESULTS AND DISCUSSION

To measure the electroporation, a time sequence of images was taken using the fluorescent microscope at a frequency of 2Hz. From these images, the intensity of each cell was measured by counting the pixel values of all the pixels in an area 20x20 micron centered on each cell. Since the fluorescent dye shows decay even without exposing the cells to an electrical field, this natural decay was first measured. The measurement shows that the mean natural

decay time is 141.5. Therefore, the natural fluorescent decay is ignorable for electroporation phenomenon occurring in 20 seconds.

The intensities of groups of stationary cells were also measured when they were exposed to the electrical field. In all experiments, the electrical field was switched on five seconds after image acquisition started. The intensity of the brightest cell in each measurement is normalized to 1, and the intensities of the other cells are normalized according to the maximum starting intensity relative to the brightest cell. The measurements were repeated for amplitudes of 5V, 3V and 1V and the corresponding results are shown in Figure 3, Figure 4 and Figure 5, respectively. The intensity plots show that for $U=5V$, the cells are electroporated within ~ 10 seconds, much faster than the natural decay of the fluorescent compound. The results show promising performance of the electric microchannel in electroporation when all the targeted cells are fully electroporated with the operational voltage as low as 5 V. Electroporation for $U=3V$ does not occur for all cells, which is likely the result of differences in individual cell physiology. Also clearly visible in the intensities at $U=3V$ electroporation, is the increase in intensity after the electric field has been turned on. This is attributed to an increase in cell size at the first moments. As the cell is electroporated, the fluorescent dye flows out, and the intensity drops sharply.

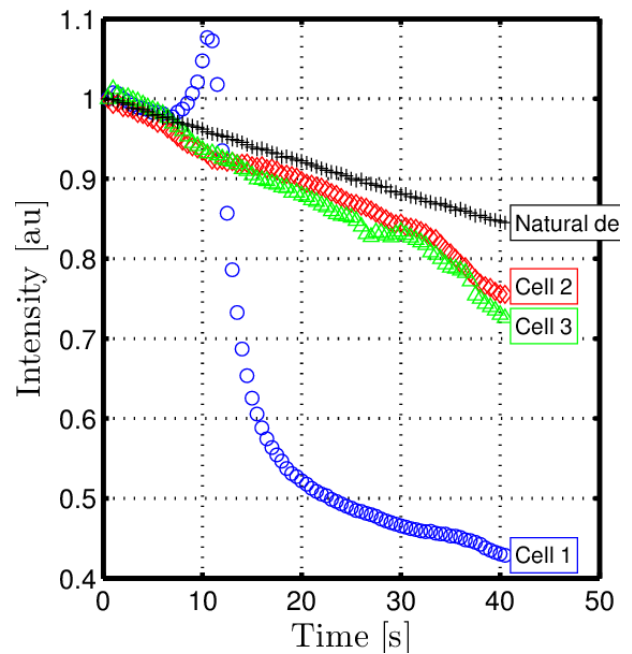


Figure 4 Electroporation of three target cells with operational voltage of $U=3V$.

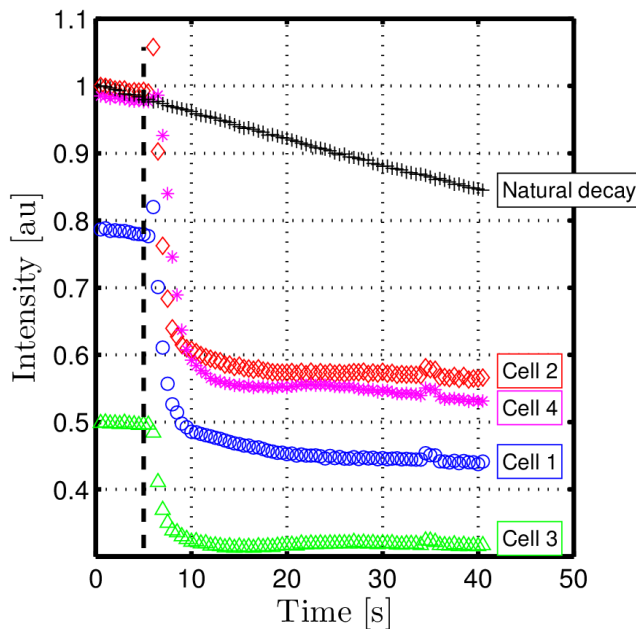


Figure 3 Electroporation of four target cells with operational voltage of $U=5V$. Electric field turned on at $t=5$ s.

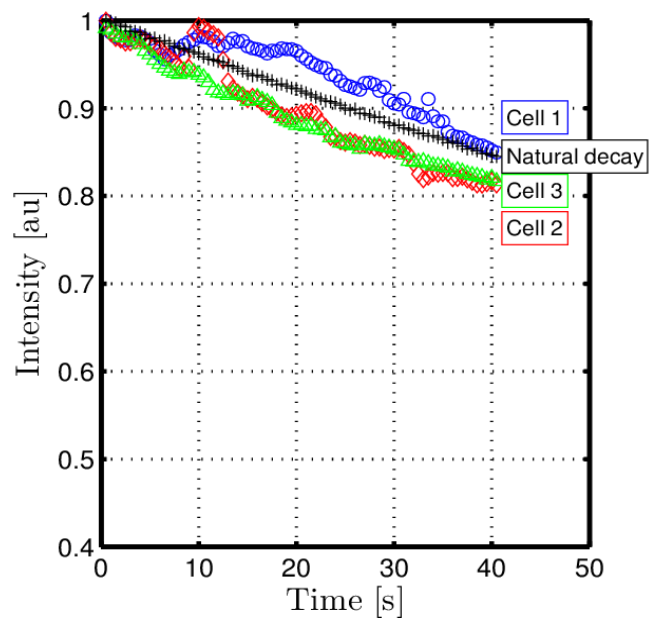


Figure 5 Electroporation of three target cells with operational voltage of $U=1V$.

The results presented here are samples to show the application of the electro-microchannel in electrical cell manipulation mechanisms. It is a promising approach to analyze behavior of single cells under electrical configurations. It should be noted that the capability of the proposed methodology is not limited to mammalian cells with relatively larger sizes. For electrical manipulation of smaller bio-samples, for example bacteria, ITO-coated cover slip, as one sample is seen in Figure 1, enables high magnification microscopic analysis. Moreover, the geometry customization of electrodes in deposition of ITO makes non-uniform electric fields in the microchannel. If such step is taken toward development of the chip, a broad range of cell treatments based on dielectrophoresis will be also achievable. Customized patterning of polyimide with no extra cost is another possibility toward integration and customization of the electro-fluidic channel in other on-chip cell manipulation systems.

Our experiments show the usefulness of the microfluidic chips created by this method, although there remains room for improvement by, for example, switching to thinner ITO-coated cover slips. Such improvements should allow higher microscopy magnifications to be used, allowing smaller cells to be imaged effectively.

5 CONCLUSION

In conclusion, we presented a novel method of fabricating microfluidic chips. This method is easy, low-cost and primarily suitable for rapid prototyping. It also combines the ability to generate an electrical field within the channel with the ability to monitor the channel contents in-situ using microscopy techniques. The results show feasibility of the proposed methodology to be applied into analysis of single cell electroporation. More developments of the proposed electro-microchip are achievable by customizing ITO-coatings and polyimide cutting patterns. These developments will enable integration of the chip with other on-chip apparatus.

REFERENCES

- [1] J.-C. Yoo, G.-S. La, C. J. Kang, and Y.-S. Kim, "Microfabricated polydimethylsiloxane microfluidic system including micropump and microvalve for integrated biosensor," *Current Applied Physics*, vol. 8, no. 6, pp. 692–695, Oct. 2008.
- [2] H. W. Hou, A. A. S. Bhagat, A. G. L. Chong, P. Mao, K. S. W. Tan, J. Han, and C. T. Lim, "Deformability based cell margination--a simple microfluidic design for malaria-infected erythrocyte separation.," *Lab on a chip*, vol. 10, no. 19, pp. 2605–13, Oct. 2010.
- [3] F. T. G. van den Brink, E. Gool, J.-P. Frimat, J. Bomer, A. van den Berg, and S. Le Gac, "Parallel single-cell analysis microfluidic platform.," *Electrophoresis*, vol. 32, no. 22, pp. 3094–100, Nov. 2011.
- [4] a V Govindarajan, S. Ramachandran, G. D. Vigil, P. Yager, and K. F. Böhringer, "A low cost point-of-care viscous sample preparation device for molecular diagnosis in the developing world; an example of microfluidic origami.," *Lab on a chip*, vol. 12, no. 1, pp. 174–81, Jan. 2012.
- [5] H. Becker and C. Gärtner, "Polymer microfabrication technologies for microfluidic systems.," *Analytical and bioanalytical chemistry*, vol. 390, no. 1, pp. 89–111, Jan. 2008.
- [6] P. Abgrall, C. Lattes, V. Conédéra, X. Dollat, S. Colin, and A. M. Gué, "A novel fabrication method of flexible and monolithic 3D microfluidic structures using lamination of SU-8 films," *Journal of Micromechanics and Microengineering*, vol. 16, no. 1, pp. 113–121, Jan. 2006.
- [7] L. Brown, T. Koerner, J. H. Horton, and R. D. Oleschuk, "Fabrication and characterization of poly(methylmethacrylate) microfluidic devices bonded using surface modifications and solvents.," *Lab on a chip*, vol. 6, no. 1, pp. 66–73, Jan. 2006.
- [8] S. Metz, R. Holzer, and P. Renaud, "Polyimide-based microfluidic devices.," *Lab on a chip*, vol. 1, no. 1, pp. 29–34, Sep. 2001.
- [9] J. Kim and X. Xu, "Excimer laser fabrication of polymer microfluidic devices," vol. 15, no. 4, pp. 255–260, 2003.